Optical Properties of TiO_2 Thin Films Grown by PLD

V. N. Cancea[1], V. Ion[2], M. Filipescu[2], M. Dinescu[1,2]

[1]Department of Physics, University of Craiova 200585, Romania

[2]Department of Lasers, National Institute for Lasers, Plasma and Radiation Physics, P.O. Box MG 16, RO-077125 Magurele-Bucharest, Romania

Abstract

Titanium dioxide thin films have been grown by pulsed laser deposition (PLD) under a fine tuning of the deposition parameters, such as the substrate temperature, gas pressure, or the application of special treatments, e.g. RF-plasma assistance conditions. The main concern during the deposition process/treatments has been to obtain a high reproducibility and well defined optical and topographic properties. The emerging TiO_2 thin films have been analyzed with respect to the above mentioned properties by Atomic Force Microscopy (AFM) and Spectroscopic Ellipsometry (SE).

Keywords: TiO_2 thin films; Pulsed Laser Deposition; Spectroscopic Ellipsometry; Atomic Force Microscopy.

1 Introduction

PLD is one of the most promising techniques for the formation of complex oxide heterostructures, super-lattices, and well controlled interfaces [1]. This technique generally enables the deposition of highly dense films and has proven its efficiency in growing oxides of complex stoichiometry. An unwanted aspect of PLD [2] is the amount of particles being ejected during the laser-target interaction and thus causing local thin film damage. Numerous variations of the conventional PLD setup have been designed to diminish this behavior, like an off-axis geometry [3], a double laser pulse approach [4] and so on. An important improvement resulted from the optimization of conventional PLD process in terms of material characteristics, laser parameters, substrate properties, and process assisting.

Titanium dioxide has been proven to be an effective material for applications such as photocatalysis [5]–[7], dye sensitized solar cells [8, 9], heterogeneous catalysis [6, 10], or self-cleaning/antifogging surface coatings [11]. TiO_2 thin films became of renewed interest due to their chemical, electrical, and optical properties [12]–[14]. In the thin film form, TiO_2 is used for instance at photon harvesting in photovoltaic applications [9, 15] and, moreover, is expected to be used as an electrode for solar power generation [16].

Titanium dioxide is especially renowned for its biomedical applications. Among these, we highlight the incorporation of an increasing amount of TiO_2 on phosphate-based glasses, which was reported to lead to enhanced gene expression and bone-forming capacity of such glasses [17] or to be effective in reducing glass degradation and enhancing

cytocompatibility in terms of MG63 cell attachment, viability, proliferation, and bone marker expression [18]. Another interesting application resides in (UV irradiated) TiO_2 whisker-based delivery of anticancer drugs as a promising approach in cancer therapy [19]. Moreover, several in vitro and in vivo studies showed the effect of coating composition on Ti surface: deposited rutile and anatase compared to natural TiO_2 show enhanced bone-like precipitation at the surface in simulated body fluids [20, 21].

Growth of TiO_2 thin films by PLD has been studied in various contexts [22]–[24]. Along this line, here we analyze the control over the substrate nature and various PLD deposition parameters, such as the substrate temperature, the gas pressure, the application of special treatments, e.g. RF-plasma assistance, in order to grow TiO_2 thin films with relatively high reproducibility and well defined optical and topographic properties. In view of this, we have grown by PLD technique several TiO_2 thin films under a fine tuning of the above mentioned conditions and then analyzed the resulting samples by means of AFM and SE.

2 Experimental

2.1 2.1 Pulsed Laser Deposition

The TiO_2 thin films are obtained by PLD technique. The beam from a pulsed ArF excimer laser system working at a wavelength of 193 nm was focused through a spherical lens on the target at 45° incidence angle [25]–[28], with the laser fluence of 3.4 J/cm^2. In order to achieve a uniform ablation, the TiO_2 ceramic target was simultaneously rotated and translated [29]. The laser spot size was measured to be 0.7 mm^2. The deposition process was carried out at different substrate temperatures, from room temperature (RT), 21° C, to 600° C. Some of the samples were deposited in vacuum and the others in the presence of oxygen at 0.01 mbar. The substrates used were placed at a distance of 4 cm from the target and the number of laser pulses was fixed at 80.000. Two types of substrates were used: double polished Si(100) transparent in the IR range and glass (BK7). The addition of a radio-frequency plasma discharge (13.56 MHz, CESAR 1310 power supply) to the PLD system combines the advantages of conventional PLD with "in situ" enhancement of the reactivity on the substrate due to the presence of an excited, ionized beam of oxygen atoms produced by the RF discharge (RF power = 100 W) [30]. The deposition parameters are summarized in Table 1.

TiO_2 sample	Substrate	P (mbar)	$T_{\text{substrate}}$ (°C)	P_{RF} (W)
1223	Glass+Si photoresist	10^{-6}	RT	0
1224	Glass	10^{-6}	300	0
1225	Glass	10^{-6}	600	0
1226	Glass	0.01 O_2	RT	0
1227	Si(100)+quartz	0.01 O_2	RT	0
1228	Glass	0.01 O_2	300	0
1229	Glass	0.01 O_2	600	0
1230	Si(100)+glass	0.01 O_2	RT	100
1231	Glass	0.01 O_2	600	100
1232	Glass	0.01 O_2	300	100

Table 1: Experimental setup for growth of TiO_2 thin films by PLD.

2.2 Atomic Force Microscopy

The AFM images have been obtained with an XE-100 Park Systems microscope is used for surface topography. The maximum horizontal scan range for this instrument is 50×50 $(\mu\text{m})^2$ while the maximum vertical movement is 12 μm.

2.3 Spectroscopic Ellipsometry

Optical measurements are done with a Woollam Variable Angle Spectroscopic Ellipsometer (VASE) system, equipped with an HS-190 monochromator. Spectroscopic ellipsometry is a non-destructive experimental technique used to detect the change in the polarization of a light beam reflected or transmitted from a surface sample. The polarization change is represented as the change in amplitude ratio Ψ and change in phase shift Δ, respectively between the p- and s- components of the light beam's electric field. These two parameters are defined via the ratio between the Fresnel reflection coefficients R_p and R_s respectively corresponding to the polarizations p and s of the electric fields parallel and respectively orthogonal to the incidence plane:

$$\rho = \frac{R_\text{p}}{R_\text{s}} = (\tan\Psi)\exp(\text{i}\Delta). \tag{1}$$

The measured response in ellipsometry depends on the optical properties and thickness of individual materials [31, 32].

At the same time, SE is a comparative technique in the sense that after a sample is measured, an optical model is constructed to describe that precise sample. The model is used to calculate the predicted response from Fresnel's equations (theoretical curves for the parameters Psi Ψ and Delta Δ), which endows each material with thickness and optical constants. The calculated values are then compared to the experimental data. Finding the best match between the model and the experiment is typically achieved through regression. An estimator, like the Mean Squared Error (MSE), is used to quantify the difference between curves. The unknown parameters are allowed to vary until the minimum MSE is reached. The best answer corresponds to the lowest MSE. In the case of thin films deposited by various techniques on a collecting material the optical model is usually composed of a chosen number of layers of material [31, 32]. More precisely, for each sample the layers associated with the optical model comprise the collecting substrate, the deposited TiO_2 thin film, and a surface (roughness layer). The composition of the rough layer was approximated to 50% TiO_2 and 50% air (voids), for ease of calculation.

The experimental data of Psi and Delta have been measured with a Woollam V-VASE spectroscopic ellipsometer equipped with a HS-190 monochromator in the spectral range of 250 to 1700 nm, in steps of 2 nm, and at an incident angle of the light beam of 70°. The transmission curves have been measured with the same device, but at an incident angle of 90° with respect to the external layer.

3 Results and discussions

AFM images, scanned on large areas (20×20 $(\mu\text{m})^2$), for thin films grown by PLD in vacuum, without RF-plasma assistance, at different temperatures, show the good quality of the surface. These films are rather smooth, with few small grains and without pores, with RMS (root-mean-square) values of the roughness ranging within 1–2 nm (see Fig. 1).

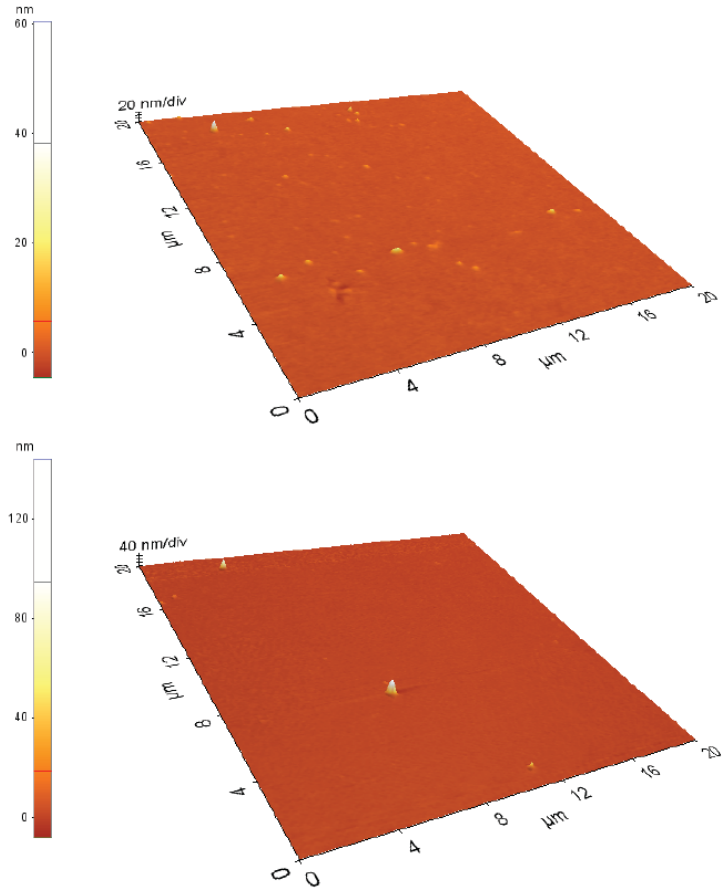

Figure 1: AFM imaging on a 20×20 $(\mu m)^2$ scanned area for TiO_2 thin films grown by PLD in vacuum, without RF: (a) up — sample 1223 at RT (RMS 0.9 nm); (b) down — sample 1225 at 600° C (RMS 1.9 nm).

Optical transmission curves for all the TiO_2/glass thin films deposited by laser ablation at various parameters (substrate temperature, oxygen pressure, RF-plasma assistance), in agreement with Table 1, are represented in Fig. 2. Analyzing the above figure, we can classify the samples according to the values of the transmittance into three classes. The first class corresponds to the smallest values (maximum 0.2) of the transmittance and contains samples 1223, 1224, and 1225, all deposited in vacuum and in absence of RF power, but at a substrate temperature varying from 25° C (RT) to 600° C. All these three samples are practically opaque in the visible and near infrared spectrum, although one can observe a slight increase of the transmittance with the substrate temperature. The second class is characterized by medium values of the transmittance (between 0.2 and 0.8) and includes samples ranging from 1226 to 1229, all deposited in the presence of a background gas (oxygen at 0.01 mbar), but without RF discharge. The third class displays the highest values of the transmittance (above 0.9) and comprises samples 1230, 1231, and 1232, all deposited in the presence of oxygen at 0.01 mbar and with RF-plasma assistance (P_{RF}=100 W). Thus, we can conclude that TiO_2 thin films deposited by laser ablation with improved optical properties, like transparency with respect to the visible and near infrared spectrum, can be obtained by oxygen admission within the reaction chamber and especially by the application of an additional "in situ" RF treatment. On the other hand, it is interesting to notice that there appear two pairs of samples, (1226,1227)

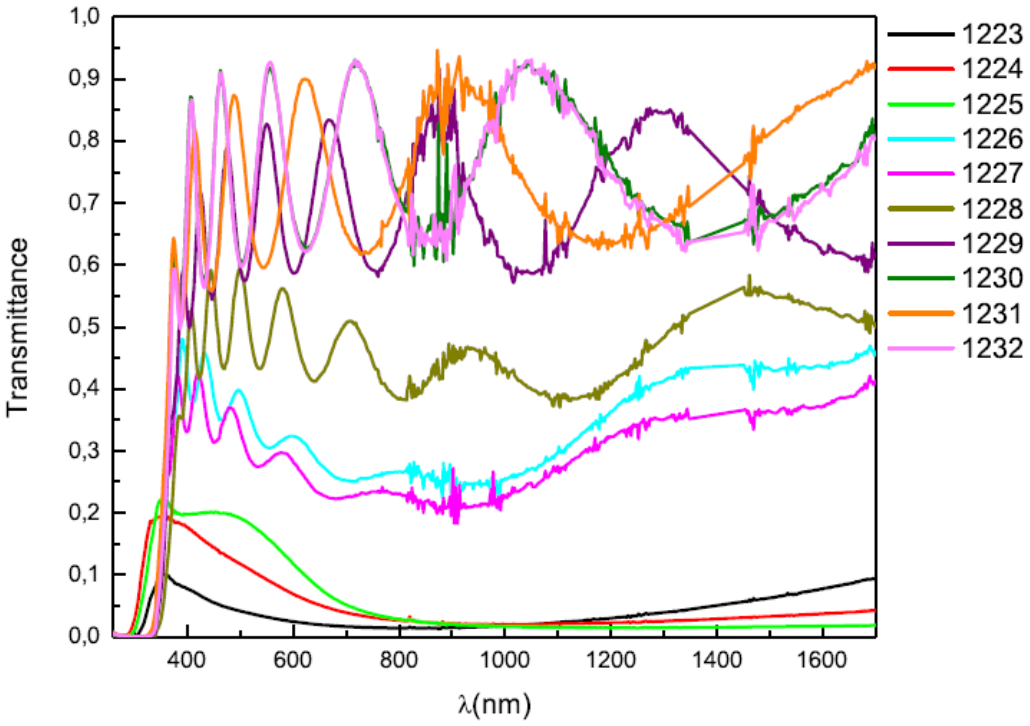

Figure 2: Transmission curves for the TiO_2/glass samples grown by PLD and by RF-PLD.

and (1230,1232), with similar curve shapes and near or almost overlapping values. This means that the reproducibility of PLD experiments for TiO_2 thin film growth is favored by implementing special "treatments" like presence of oxygen during deposition or RF plasma discharge.

Special attention was paid to the influence of the substrate on the optical properties of TiO_2 thin films grown by PLD. In view of this, we analyze by SE two samples grown under the same conditions (RT, oxygen at 0.01 mbar, P_{RF}=100 W), but on different substrates: silicon and respectively glass (1230/Si and 1230/glass). The calculation of the refractive index (n), thickness, and roughness of the two investigated thin films from the recorded experimental data starts from the identification of a specific spectral range (400–1150 nm), where TiO_2 is practically transparent ($k = 0$). The refractive index (n) of the TiO_2 films was modeled using the two-term Cauchy dispersion formula (Cauchy fitting) $n(\lambda) = A_n + B_n/\lambda^2$ [32], with A_n and B_n the Cauchy coefficients. The optical model used for fitting the experimental data takes into account: (a) for sample 1230/Si the silicon substrate, a layer of native oxide of silicon of approximately 3 nm in thickness, the TiO_2 thin film, and a roughness layer (taken as a Bruggemann Effective Medium Approximation — BEMA, of equal air/material densities, 50%-50%); (b) for sample 1230/glass the glass substrate, the TiO_2 thin film, and a roughness layer (BEMA 50%-50%). The values of the optical constants of the composing layers have been taken from the literature for Si [33] and respectively from the spectroscopic ellipsometer database (BK7 for glass). The resulting values of the Cauchy parameters A_n and B_n together with thickness and roughness values for the two investigated samples, and also the MSE results, are given in Table 2. We notice that each parameter displays close values for both samples and, in addition, the values for roughness are close to those emerging from AFM measurements.

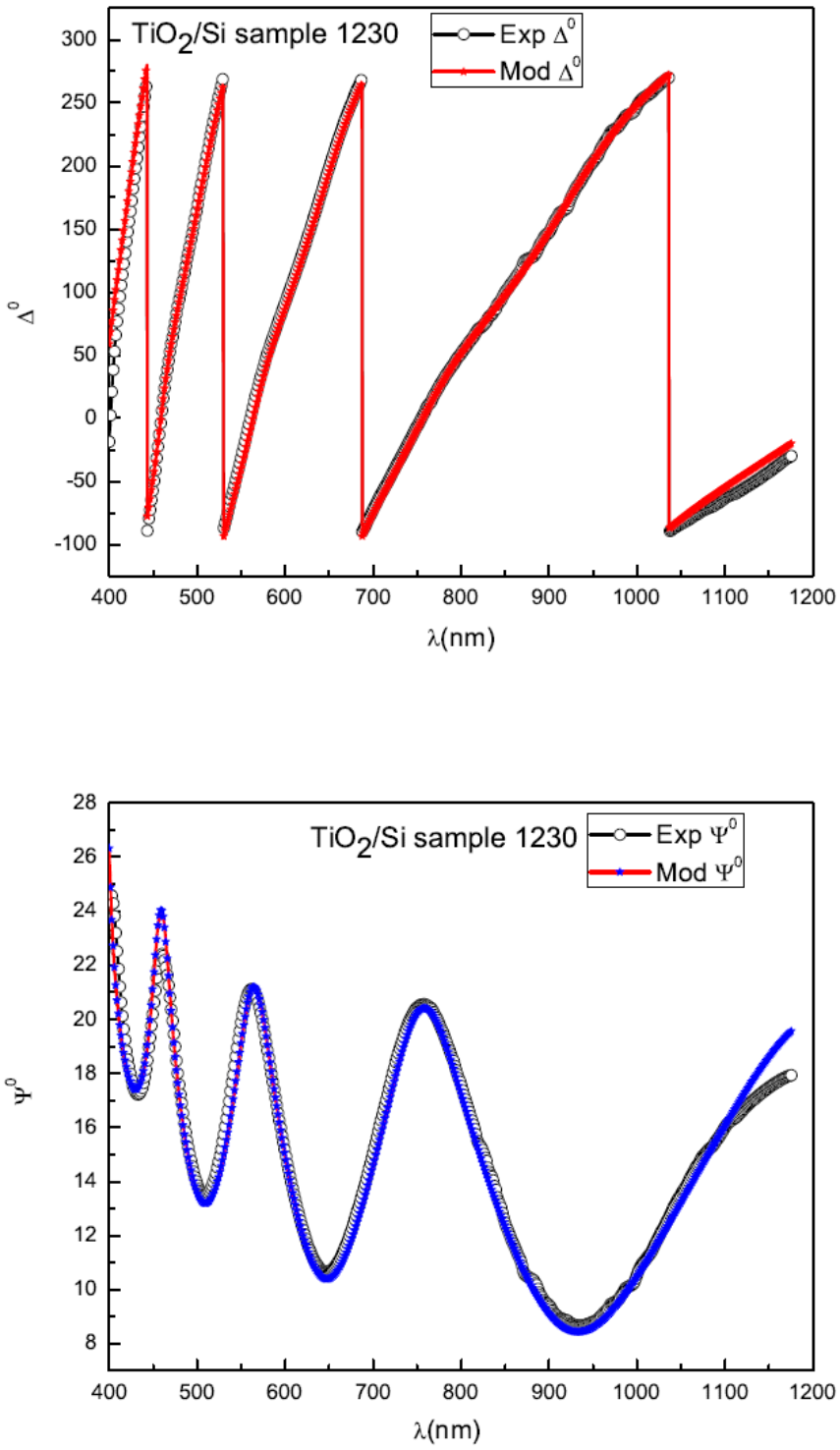

Figure 3: Experimental and Cauchy-modeled curves for the parameters Δ (up) and Ψ (down) for TiO_2 sample 1230/Si.

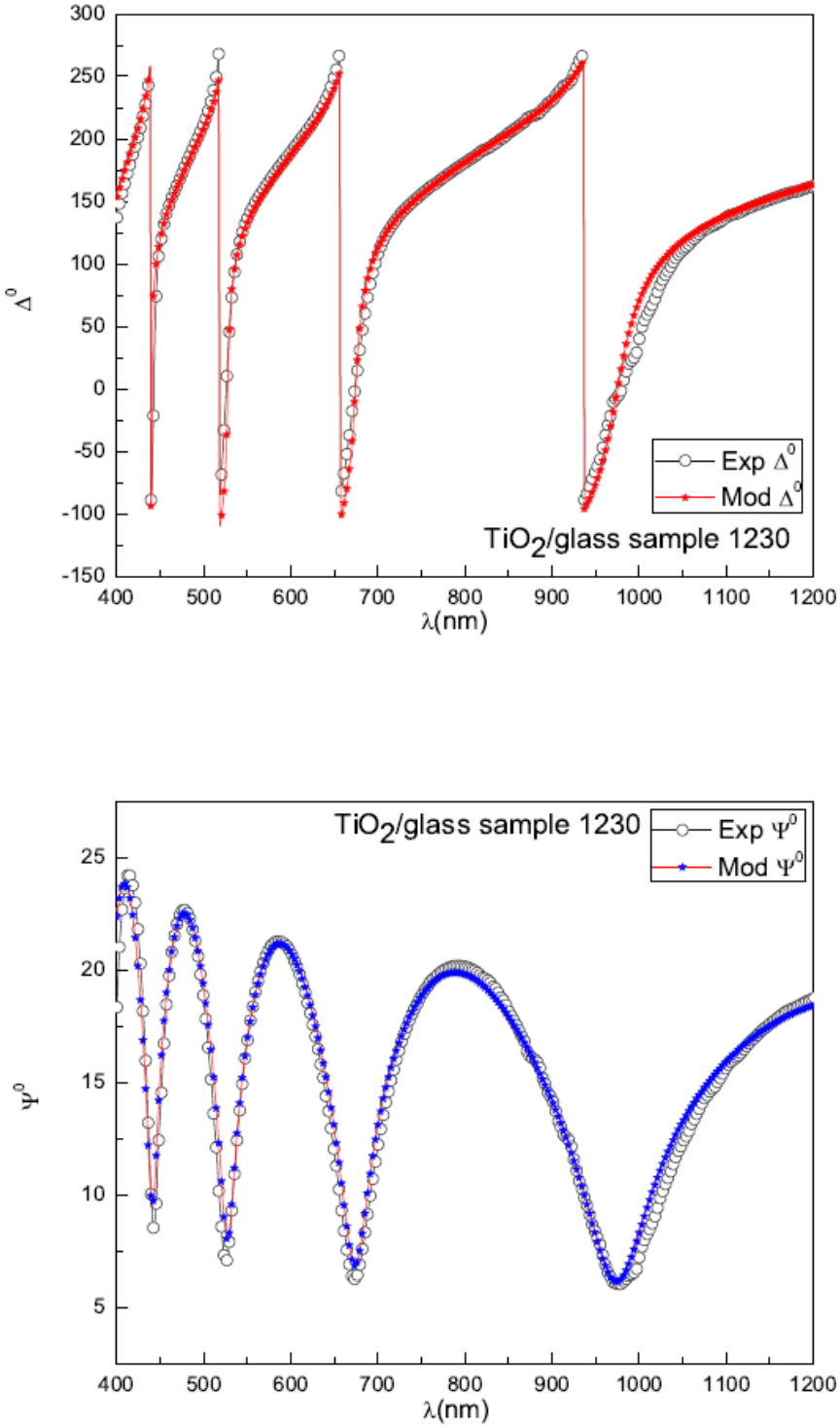

Figure 4: Experimental and Cauchy-modeled curves for the parameters Δ (up) and Ψ (down) for TiO_2 sample 1230/glass.

Substrate	Thickness (nm)	Roughness (nm)	A_n	B_n	MSE
Si(100)	413.538 ± 0.524	0.424 ± 0.232	2.3437 ± 0.00226	0.064031 ± 0.000482	26.46
Glass	444.726 ± 0.546	2.023 ± 0.247	2.2871 ± 0.0024	0.065593 ± 0.000458	24

Table 2: Cauchy parameters for TiO_2 samples 1230/Si and 1230/glass.

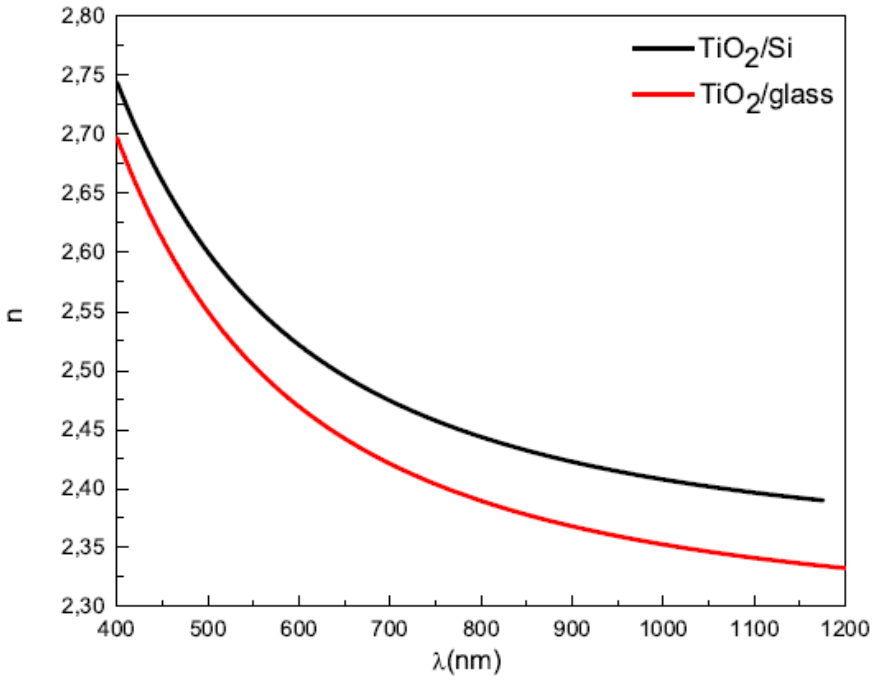

Figure 5: Dependencies of n for TiO_2 samples 1230/Si and 1230/glass.

Fig. 3 and Fig. 4 present the experimental curves and those obtained by Cauchy fitting method for the parameters Δ and Ψ related to each sample. It is clear that each of the two sets of curves behaves similarly (they almost overlap), so the optical model is correct.

In Fig. 5 are given the curves for the refractive index n for both samples. The refractive index (n) values for TiO_2 deposited by PLD in the same conditions, but on different substrates (Si and glass), are high and relatively close for the entire investigated spectral range and, moreover, comparable with the results from the literature [34].

4 Conclusions

The general conclusion of the analysis of TiO_2 thin films grown by PLD and RF plasma-assisted PLD in terms of spectroscopic ellipsometry is that these deposition methods are suitable for obtaining good transparency properties within visible and near infrared spectrum. Beside, thin films displaying large values of the refractive index ($n > 2.3$) can be obtained using different substrates, which proves once more that the laser ablation is a reliable and reproducible deposition method.

Acknowledgments

One of the authors (V.N.C.) acknowledges partial support from the doctoral contract 336/9/B/30.09.2011 with the University of Craiova.

References

[1] H. M. Christen, G. Eres, J. Phys.: Condens. Matter **20** (2008) 264005

[2] S. Heiroth, J. Koch, T. Lippert, A. Wokaun, D. Günther, F. Garrelie, M. Guillermin, J. Appl. Phys. **107** (2010) 014908

[3] B. Holzapfel, B. Roas, L. Schultz, P. Bauer, G. Saemannischenko, Appl. Phys. Lett. **61** (1992) 3178–3180

[4] P. Caminat, E. Valerio, M. Autric, C. Grigorescu, O. Monnereau, Thin Solid Films **453/454** (2004) 269–272

[5] A. Fujishima, K. Honda, Nature **238** (1972) 37–38

[6] H. Lin, C. P. Huang, W. Li, C. Ni, S. I. Shah, Y. H. Tseng, Appl. Catal., B **68** (2006) 1–11

[7] H. Lin, A. K. Rumaiz, M. Schulz, D. Wang, R. Rock, C. P. Huang, S. I. Shah, Mater. Sci. Eng., B **151** (2008) 133–139

[8] B. Oregan, M. Gratzel, Nature, **353** (1991) 737–740

[9] A. Hagfeldt, M. Gratzel, Acc. Chem. Res. **33** (2000) 269–277

[10] M. Valden, X. Lai, D. W. Goodman, Science **281** (1998) 1647–1650

[11] T. Watanabe, A. Nakajima, R. Wang, M. Minabe, S. Koizumi, A. Fujishima, K. Hashimoto, Thin Solid Films **351** (1999) 260–263

[12] S. K. Zhang, T. M. Wang, G. Xiang, C. Wang, Vacuum **62** (2001) 361–366

[13] R. Paily, A. DasGupta, N. DasGupta,T. Ganguli,M. L. Kukreja, Thin Solid Films **462/463** (2004) 57–62

[14] Lei Zhao, Jian-she Lian, Trans. Nonferrous Met. Soc. China **17** (2007) 772–776

[15] S. I. Kitazawa, Y. Choi, S. Yamamoto, T. Yamaki, Thin Solid Films **515** (2006) 1901–1904

[16] T. Nakamara, T. Ichitsubo, E. Matsubara, A. Muramatsu, N. Sato, H. Takahashi, Acta Mater. **53** (2005) 323–329

[17] E. A. Abou Neel, W. Chrzanowski, J. C. Knowles, Acta Biomater. **4** (2008) 523–534

[18] E.A. Abou Neel, T. Mizoguchi, M. Ito, M. Bitar, V. Salih, J.C. Knowles, Biomaterials **28** (2007) 2967–2977

[19] Q. Li, X. Wang, X. Lu, H. Tian, H. Jiang, G. Lv, D. Guo, C. Wu, B. Chen, Biomaterials **30** (2009) 4708–4715

[20] B. Feng, J. Weng, B. C. Yang, S. X. Qu, X. D. Zhang, Biomaterials **24** (2003) 4663–4670

[21] T. Jinno, S. K. Kirk, S. Morita, V. M. Goldberg, J. Arthroplasty **19** (2004) 102–109

[22] D. Luca, D. Macovel, C. M. Teodorescu, Surf. Sci. **600** (2006) 4342–4346

[23] N. E. Stankova, I. G. Dimitrov, T. R. Stoyanchov, P. A. Atanasov, Appl. Surf. Sci. **254** (2007) 1268–1272

[24] N. E. Stankova, P. A. Atanasov, A. O. Dikovska, I. G. Dimitrov, G. Socol, I. N. Mihailescu, SPIE **5830** (2005) 60–64

[25] P. Verardi, M. Dinescu, F. Craciun, Appl. Surf. Sci. **154–155** (2000) 514–518

[26] F. Craciun, P. Verardi, D. Brodoceanu, M. Morar, C. Galassi, C. Grigoriu, M. Dinescu, Mater. Sci. Semicond. Proc. **5** (2002) 227–232

[27] I. Vrejoiu, D. G. Matei, M. Morar, G. Epurescu, A. Ferrari, M. Balucani, G. Lamedica, G. Dinescu, C. Grigoriu, M. Dinescu, Mater. Sci. Semicond. Proc. **5** (2002) 253–257

[28] L. Cultrera, P. Miglietta, A. Perrone, J. Alloy Compd. **504S** (2010) S399–S404

[29] N. Arnold, D. Bäuerle, Appl. Phys. A **68** (1999) 363–367

[30] M. Filipescu, N. Scarisoreanu, V. Craciun, B. Mitu, A. Purice, A. Moldovan, V. Ion, O. Toma, M. Dinescu, Appl. Surf. Sci. **253** (2007) 8184–8191

[31] H. G. Tompkins, E. A. Irene (Eds.), Handbook of Ellipsometry, William Andrew, Inc., Springer Verlag, 2005

[32] H. Fujiwara, Spectroscopic ellipsometry: principles and applications, John Wiley & Sons Ltd., 2007

[33] C. M. Herzinger, B. Johs, W. A. McGahan, J. A. Woollam, W. Paulson, J. Appl. Phys. **83** (1998) 3323–3336

[34] S. Tanemura, L. Miao, P. Jin, K. Kaneko, A. Terai, N. Nabatova-Gabain, Applied Surf. Sci. **212–213** (2003) 654–660